

# Fractional Fourier Transform based Monopulse Radar for Combating Jamming Interference

Sherif A. Elgamel<sup>#1</sup>, John J. Soraghan<sup>#2</sup>

<sup>#</sup>Department of Electronic and Electrical Engineering, University of Strathclyde  
204 George Street, G1 1XW, Glasgow, UK

<sup>1</sup> sherifelgamel73@gmail.com

<sup>2</sup> j.soraghan@eee.strath.ac.uk

**Abstract**— Monopulse radars are used to track a target that appears in the look direction beam width. The distortion produced when manmade high power interference (jamming). Jamming scenarios are achieved by introducing high power interference to the radar processor through the radar antenna main lobe (main lobe interference) or antenna side lobe (side lobe interference). This leads to errors in the target tracking angles that may cause target mistracking. A new monopulse radar structure is presented in this paper which offers a solution to this problem. This structure is based on the use of optimal Fractional Fourier Transform (FrFT) filtering. The proposed system configurations with the optimum FrFT filters is shown to reduce the simulated interfered signal and improve the signal to noise ratio (SNR) in the processors outputs in both processor using the proposed monopulse structure.

## I. INTRODUCTION

Monopulse radars are commonly used in target tracking because of their angular accuracy [1]. They provide superior angular accuracy and less sensitivity to fluctuation in the radar cross section (RCS) of the target compared to other types of tracking radars [2]. These radars are affected by different types of interference which affects the target tracking process and may lead to inaccurate tracking [3-5].

A jamming scenario where high power manmade interference is introduced to the radar processor through the antenna main lobe (main lobe interference) or through antenna side lobe (side lobe interference) is illustrated in Fig 1. The resultant distortion due to this interference will affect the induced error voltage which responsible to drive the antenna towards the target and consequently may lose tracking. Adaptive monopulse processors can be used to decrease the effect of the noise interference[6]. In this paper an optimal fractional Fourier transform based monopulse radar is presented. The new radar is demonstrated to reduce the interference due to main lobe or side lobe interference signals compared to that possible using the conventional monopulse radar..

The paper is organized as follows: monopulse processors are introduced in section II. Section III introduces the fractional Fourier transform (FrFT) and explains how the optimum chose of FrFT order is made and also how to calculate the peak position sample of a chirp signal in optimum FrFT domain.

The FrFT based monopulse radar is shown in section IV.

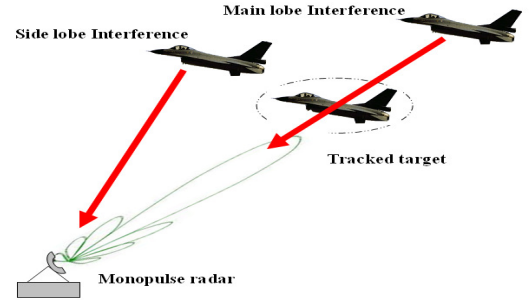


Fig 1. Jamming scenarios for Monopulse radar.

In section V a set of simulation results is presented for the new monopulse structure using the proposed filtering technique in the optimum FrFT show the reduction in the interfered signal. Section VI concludes the paper.

## II. MONOPULSE RADAR PROCESSORS

### A. Monopulse Radar processors

1) The conventional processor is a non adaptive system comprising two sets of weights set to the sum and difference steering vectors defined as [7]:

$$w_{\Sigma} = a(\nu_l), \quad w_{\Delta} = \left. \frac{\partial a(\nu)}{\partial \nu} \right|_{\nu_l} \quad (1)$$

where  $a(\nu)$  is the centre phase normalized steering vector in the look direction,  $N$  is the number of antenna,  $\nu$  is the spatial steering frequency, and  $\nu_l$  is the spatial steering frequency snapshot at time instant  $l$ .

2) The spatial processor is an adaptive system comprising an adaptive sum and difference beams formed by applying sum and difference gain constraints in the look direction, the sum and difference weights may be written in the following form [7]:

$$w_{\Sigma} = \frac{R_x^{-1} \nu_{\Sigma}}{\nu_{\Sigma}^H R_x^{-1} \nu_{\Sigma}}, \quad w_{\Delta} = \frac{R_x^{-1} \nu_{\Delta}}{\nu_{\Delta}^H R_x^{-1} \nu_{\Delta}} \quad (2)$$

where  $R_x$  is the covariance matrix of the input data,  $\nu_{\Sigma}$  and  $\nu_{\Delta}$  are the spatial steering frequency for the sum and difference channel respectively and  $H$  indicates the Hermitian.

3) The sum and difference outputs are given in terms

of the respective processors,

$$z_{\Sigma}(l) = w_{\Sigma} \mathbf{x}(l), \quad z_{\Delta}(l) = w_{\Delta} \mathbf{x}(l) \quad (3)$$

where  $\mathbf{x}(l)$  is the  $N \times 1$  spatial snapshot at time instant  $l$ . The real part of the ratio of difference to sum outputs is known as the error voltage defined as [6, 7]

$$\varepsilon_v(l) = \Re \left\{ \frac{z_{\Delta}(l)}{z_{\Sigma}(l)} \right\} \quad (4)$$

This error voltage conveys purely directional information that must be converted to an angular form via a mapping function [6].

4) Output interference-to-noise ratio (*OINR*) [8, 9] is defined as the ratio of the processor output power to the noise power.

$$OINR = \frac{E\{|z_i|^2\}}{\sigma_n^2} \quad (5)$$

where  $z_i$  is the output of the processor when only interference is present and  $\sigma_n^2$  is the noise power. *OINR* is used to compare the mitigation performance for the different monopulse processors. A lower *OINR* value implies improved mitigation performance.

### III. FRACTIONAL FOURIER TRANSFORM

The fractional Fourier transform (FrFT) is the generalized formula for the Fourier transform that transforms a function into an intermediate domain between time and frequency. The signals with significant overlap in both the time and frequency domain may have little or no overlap in the fractional Fourier domain. The fractional Fourier transform of order  $a$  of an arbitrary function  $x(t)$ , with an angle  $\alpha$  is shown in Fig 2, is defined as [10]:

$$X_{\alpha}(t_a) = \int_{-\infty}^{\infty} x(t) K_{\alpha}(t, t_a) dt \quad (6)$$

where  $K_{\alpha}(t, t_a)$  is the transformation Kernel,  $t_a$  is the transformation of  $t$  to the  $a^{\text{th}}$  order, and  $\alpha = a\pi/2$  with  $a \in \mathfrak{R}$ .  $K_{\alpha}(t, t_a)$  is calculated from:

$$K_{\alpha}(t, t_a) = \begin{cases} \sqrt{\frac{1-j\cot\alpha}{2\pi}} e^{j\frac{t^2+t_a^2}{2}\cot\alpha - jt_a\csc\alpha} & \text{if } \alpha \text{ is not a multiple of } \pi \\ \delta(t-t_a) & \text{if } \alpha \text{ is a multiple of } 2\pi \\ \delta(t+t_a) & \text{if } \alpha + \pi \text{ is a multiple of } 2\pi \end{cases} \quad (7)$$

The optimum order value,  $a_{opt}$ , for a chirp signal may be written as [11]:

$$a_{opt} = -\frac{2}{\pi} \tan^{-1} \left( \frac{\delta f}{2\gamma \times \delta t} \right) \quad (8)$$

where  $\delta f$  is the frequency resolution ( $\delta f = F_s/N$ ),  $\delta t$  is the time resolution ( $\delta t = 1/F_s$ ),  $F_s$  is the sampling frequency, and  $\gamma$  is the chirp rate parameters.

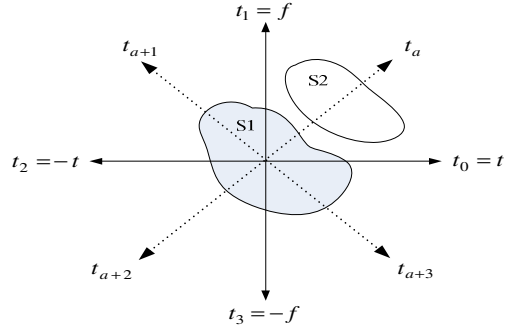


Fig 2. Signal separation in the  $a^{\text{th}}$  domain

$$\alpha_{opt} = \frac{\pi}{2} a_{opt} \quad (9)$$

Equations (8, 9) can be used to either calculate the optimum FrFT order or to estimate the chirp rate of a signal for a given FrFT order. The optimum FrFT order  $a_{opt}$  for the chirp can be computed by applying (8) as:

$$a_{opt} = -\frac{2}{\pi} \tan^{-1} \left( \frac{F_s^2 \times T}{\Delta f \times L} \right) \quad (10)$$

where  $F_s$  is the sampling frequency,  $T$  is the chirp duration,  $L$  is the number of samples in the time received window, and  $\Delta f$  is the chirp bandwidth.

The peak position  $P_p$  of a chirp signal in the FrFT domain is defined as [12]:

$$P_p = \sin(\alpha) \left[ \frac{F_{start}}{\delta f} + \frac{\Delta f (L/M_T)}{2 \times \delta f} \right] - \cos(\alpha) t_{st} \quad (11)$$

where  $M_T$  is the number of samples in the chirp signal with pulse width  $T$ , and  $t_{st}$  is the chirp start time sampling number. The peak position  $P_p$  of a chirp signal in the optimal FrFT domain can be computed by applying (11) to the radar system as:

$$P_p = \sin(\alpha_{opt}) \left[ \frac{-(\Delta f/2)}{(F_s/L)} + \frac{\Delta f (L/M_T)}{2 \times (F_s/L)} \right] - \cos(\alpha_{opt}) t_{st} \quad (12)$$

### IV. A NEW STRUCTURE OF MONOPULSE RADAR

In the proposed FrFT based monopulse radar illustrated in Fig 3, new blocks including the FrFT filtering block are introduced. A pulsed chirp signal  $c(t)$  is produced from the waveform generator.

$$c(t) = \exp(j\pi \left( \frac{F_{stop} - F_{start}}{T} \right) (t - \frac{T}{2})^2) \quad (13)$$

where  $t$  is the time,  $T$  is the chirp time duration (pulse duration),  $F_{start}$  is the chirp start frequency, and  $F_{stop}$  is the chirp stop frequency.

This is up-converted to the radar carrier frequency, amplified and passed through the duplexer to be transmitted. The down-converted received signal passes

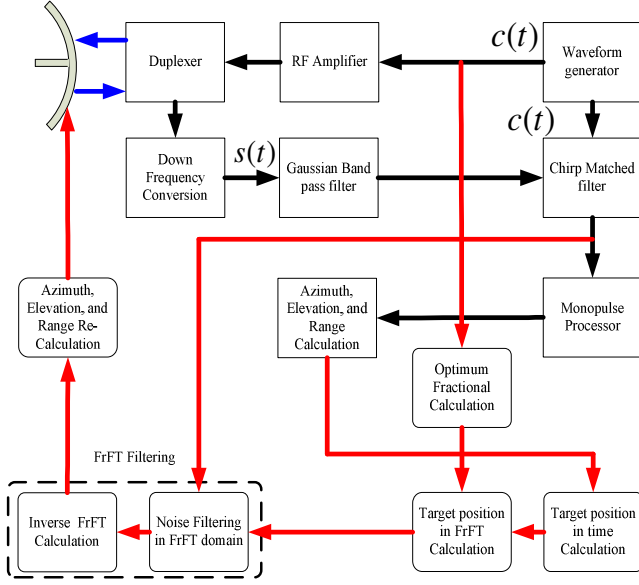


Fig 3. New structure of the proposed monopulse radar

through a band limited Gaussian filter.

The received signal  $s(t)$  may be expressed in the baseband as:

$$s(t) = \begin{cases} [Ae^{-j2\pi\phi} e^{j\pi\frac{F_{stop}-F_{start}}{T}(t-T_{start})^2} \cdot F_d] \times F_\phi & T_{start} < t < T_{start} + T \\ zero & \text{elsewhere} \end{cases} \quad (14)$$

where  $A$  is the received signal amplitude,  $\phi_o$  is a random phase shift, and  $T_{start}$  is the start time of the returned pulse, passes through a band pass Gaussian filter. The start time  $T_{start}$  depend on the target range  $R_t$ .

The mathematical model for the received signal (target chirp signal plus the additive jamming signal) assuming no system degradation) [3] is:

$$z = x + n_{jam} \quad (15)$$

where the useful signal  $x$  is the tracked target signal and the distortion signal  $n_{jam}$  is interference signal.

Barrage noise jamming  $n_{jam}$  is the most common form of hostile interference. Such interference emanates from a spatially localized source and is temporally uncorrelated from sample to sample as well as from PRI to PRI. It is modelled as the Kronecker product of a white Gaussian  $n_j(t)$  noise vector with a spatial steering vector,

$$n_{jam} = n_j(t) \otimes a(v) \quad (16)$$

where the power of each component of  $n_j(t)$  is  $\sigma_j^2$ .

The following steps are involved in the proposed algorithm that may be used to reduce the noise interference signal:

- 1) Determine the optimal fractional domain  $a_{opt}$

The optimal fractional domain  $a_{opt}$  is calculated for the tracked target signal from the information supplied from the wave generator. It can be computed by applying (8) to the radar system as:

$$a_{opt} = -\frac{2}{\pi} \tan^{-1} \left( \frac{F_s^2 \times T}{(F_{stop} - F_{start}) \times L} \right) \quad (17)$$

where  $F_s$  is the sampling frequency.

- 2) Identify the samples occupied by the target in the time domain to determine  $St_n$ .

From the target position on the return radar window, the chirp start time sampling number  $St_n$  is determined. So the target peak position in the optimum FrFT can be calculated from (12)

- 3) Calculate the peak position of the target in the FrFT domain and filtering the received data

The peak position sample and the adjacent samples (5 samples in both sides) are kept and all rest of the samples in the tracking window to be equal to zero to get the filtered data in the optimal FrFT domain  $z'$ .

- 5) Use the inverse FrFT with the known optimal order.

The filtered signal  $x'$  in the time domain is introduced by applying inverse FrFT using the same optimal operator  $a_{opt}$  to get the signal back to time domain after filtering as:

$$x' = F^{-a_{opt}}(z') \quad (18)$$

- 6) Recalculate the target information.

All the outputs signals from the  $N$  FrFT filters are then re-processed to get the target information parameters after applying the proposed filtering technique using (3) and (4) as described in section II.

## V. SIMULATION RESULTS

A monopulse radar with an array of 14 elements spaced 1/3 meters apart is simulated. The radar pulse width is 100 microseconds and the pulse repetition interval of 1.6 milliseconds using a 435 MHz carrier is employed. A 200 kHz Gaussian band pass filter exists at the front end of each of the  $N$  receivers. These are used to filter the incoming data returns prior to sampling. The incoming base band signals are sampled at 1 MHz. Also it is assumed that the radar operating range is 100:200 range bins with a starting window at 865 microseconds and a window duration of 403 microseconds. The desired target is known to exist at range bin=150 at angle 32° from the look direction with target signal to noise ratio (SNR) set to 70 dB and a Doppler frequency of 150 Hz.

### A. Simulated Data Jamming Scenario

A jamming signal with interference noise ratio (INR) set to 82 dB with two scenarios, first at angle 32° from the look direction (main beam jamming) and second at angle 62° from the look direction (side lobe beam jamming) are introduced. The jamming interference causes deviations in

the monopulse error voltages from their original values (no jamming). This distortion affects the tracking angle of the tracked target resulting in a probable mistracking outcome.

Substituting the monopulse radar parameter values into Eq (10), the order of the optimal FrFT domain  $a_{opt}$  is computed as 1.7074. Following the steps mentioned in section IV, the target in the time domain  $t_{st}$  occurs at bin 150. The target sample peak position in the optimum fractional domain is computed to exist at 205. All the samples in tracking window in the fractional domain are forced to zero except the samples from 200 to 210 (peak position sample and its five adjacent samples). The inverse FrFT with  $a_{opt}$  equal to -1.7074 transforms the signal back to time domain after filtering. The azimuth, elevation target angles and processor output can then be computed.

The processors' outputs using (3) for target SNR=70 dB is shown in Fig 4 and Fig 5 for the main lobe interference and in Fig 6 and Fig 7 for the side lobe interference, for the conventional and spatial adaptive processors respectively. In all these figures the target exists at range bin 150. Using FrFT filtering, the processors' output, in case of main lobe interference, decreases the noise level as seen in Fig 4 and Fig 5. The noise interference signal is reduced by approximately 25dB in the conventional case and by approximately 5 dBs in the case of the spatial adaptive processor. In the case of side lobe interference as shown in Fig 6 and Fig 7, the proposed FrFT filtering technique helps to decrease the noise levels by approximately 12dBs and 4dBs at the outputs of the conventional and spatial adaptive processors respectively.

Output interference-to-noise ratio  $OINR$  (7) is used to quantify the improvement. It is used to compare the mitigation performance for both monopulse processors using (5), knowing that the lowest  $OINR$  value represents the best mitigation performance.

$OINR$  values in Table I shows that the FrFT filtering technique enhances the processors mitigation due to noise for both jamming scenarios. From Table I it is observed that the  $OINR$  values for main lobe interference are always higher than those for the side lobe inference (that is clear

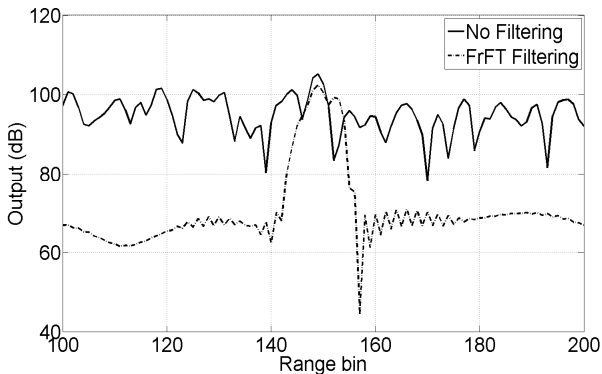


Fig 4. Conventional processor Output (main lobe)

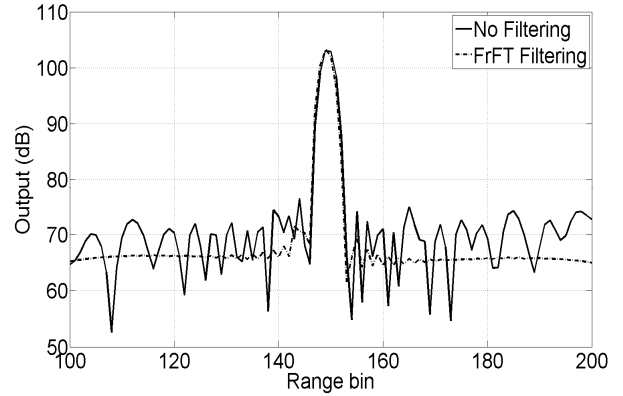


Fig 5. Spatial adaptive processor Output (main lobe)

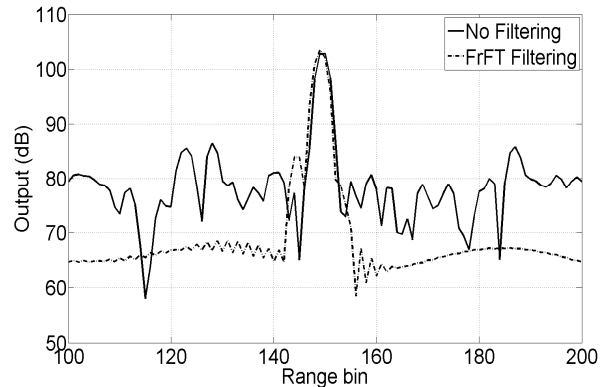


Fig 6. Conventional processor Output (side lobe)

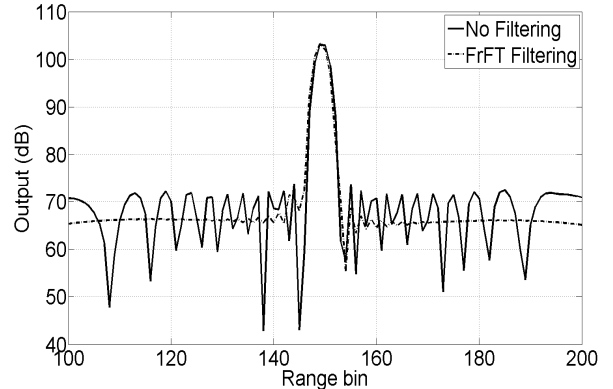


Fig 7. Spatial adaptive processor Output (side lobe)

because the distortion effect of side lobe interference is less than the main lobe interference). Also it is seen that the  $OINR$  values using FrFT filtering are always less than the  $OINR$  values without filtering (the proposed filtering technique helps to decrease the noise level for all processors in all noise interference cases). From Table 1 in case of conventional processor the  $OINR$  values are improved by approximately 15 dB and 9.7 dB for main lobe interference and side lobe interference respectively using FrFT filtering. In the case of spatial adaptive processor the  $OINR$  values are improved by approximately 9.6 dB and 9.5 dB for main lobe interference and side lobe interference respectively.

TABLE I  
OINR IN DB FOR MONOPULSE PROCESSORS

Monopulse processor	Main lobe interference	Side lobe interference
Conventional processor		
(a)No filtering	14.31	-3.3
(b)FrFT filtering	-1.33	-12.99
Spatial processor		
(a)No filtering	-19.69	-77.18
(b)FrFT filtering	-23.3	-86.75

## VI. CONCLUSION

The distortion resulting from interference appearing in the monopulse main lobe and side lobe has been investigated. The proposed FrFT based monopulse radar system configuration with the optimum FrFT filtering successfully reduces the interference noise. The proposed filtering technique helps to decrease the noise level for the studied processors in both jamming scenarios cases that the *OINR* values using FrFT filtering are always less than the *OINR* values without filtering.

## REFERENCES

- [1] R. Klemm and U. Nickel, "Adaptive monopulse with STAP," in *Radar, 2006. CIE '06. International Conference on*, 2006, pp. 1-4.
- [2] M. I. Skolnik, *Radar Handbook- Second edition*: McGraw-Hill, Inc., 1990.
- [3] S. A. Elgamel and J. Soraghan, "Target tracking enhancement using a Kalman filter in the presence of interference," in *Geoscience and Remote Sensing Symposium, 2009 IEEE International, IGARSS 2009*, 2009, pp. III-681-III-684.
- [4] S. A. Elgamel and A. H. Makaryous, "Performance of Modern Guided Systems in Presence of Jamming Signal", in *9th international conference on aerospace science and aviation technology*, Military Technical College, Cairo, Egypt, 2001.
- [5] A. D. Seifer, "Monopulse-radar angle tracking in noise or noise jamming," *Aerospace and Electronic Systems, IEEE Transactions on*, vol. 28, pp. 622-638, 1992.
- [6] Y. Seliktar, "Space- Time Adaptive Monopulse Processing." vol. PhD: Georgia Institute of Technology, 1998.
- [7] S. Yaron, B. W. Douglas, and E. J. Holder, "A space/fast-time adaptive monopulse technique." vol. 2006: Hindawi Publishing Corp., pp. 218-218.
- [8] Y. Seliktar, E. J. Holder, and D. B. Williams, "An adaptive monopulse processor for angle estimation in a mainbeam jamming and coherent interference scenario," in *Acoustics, Speech and Signal Processing, 1998. Proceedings of the 1998 IEEE International Conference on*, 1998, pp. 2037-2040 vol.4.
- [9] Y. Seliktar, D. B. Williams, and E. J. Holder, "Beam-augmented space-time adaptive processing," in *Acoustics, Speech, and Signal Processing, 1999. ICASSP '99. Proceedings., 1999 IEEE International Conference on*, 1999, pp. 2849-2852 vol.5.
- [10] C. Candan, M. A. Kutay, and H. M. Ozaktas, "The discrete fractional Fourier transform," *Signal Processing, IEEE Transactions on*, vol. 48, pp. 1329-1337, 2000.
- [11] C. Capus and K. Brown, "Short-Time fractional fourier methods for the time-frequency representation of chirp signals," *The Journal of the Acoustical Society of America*, vol. 113(6), pp. 3253-63, 2003.
- [12] R. Jacob, T. Thomas, and A. Unnikrishnan, "Applications of Fractional Fourier Transform in Sonar Signal Processing", *IETE Journal of Research*, vol. 55, pp. 16-27, 2009.